

# A Combined PET/CT Scanner for Clinical Oncology

Thomas Beyer, David W. Townsend, Tony Brun, Paul E. Kinahan, Martin Charron, Raymond Roddy, Jeff Jerin, John Young, Larry Byars, and Ronald Nutt

*PET Facility and Division of Nuclear Medicine, Department of Radiology, University of Pittsburgh, Pittsburgh, Pennsylvania; CTI PET Systems, Knoxville; and Byars Consulting, Oak Ridge, Tennessee*

The availability of accurately aligned, whole-body anatomical (CT) and functional (PET) images could have a significant impact on diagnosing and staging malignant disease and on identifying and localizing metastases. Computer algorithms to align CT and PET images acquired on different scanners are generally successful for the brain, whereas image alignment in other regions of the body is more problematic. **Methods:** A combined PET/CT tomograph with the unique capability of acquiring accurately aligned functional and anatomical images for any part of the human body has been designed and built. The PET/CT scanner was developed as a combination of a Siemens Somatom AR.SP spiral CT and a partial-ring, rotating ECAT ART PET scanner. All components are mounted on a common rotational support within a single gantry. The PET and CT components can be operated either separately, or in combined mode. In combined mode, the CT images are used to correct the PET data for scatter and attenuation. Fully quantitative whole-body images are obtained for an axial extent of 100 cm in an imaging time of less than 1 h. When operated in PET mode alone, transmission scans are acquired with dual  $^{137}\text{Cs}$  sources. **Results:** The scanner is fully operational and the combined device has been operated successfully in a clinical environment. Over 110 patients have been imaged, covering a range of different cancers, including lung, esophageal, head and neck, melanoma, lymphoma, pancreas, and renal cell. The aligned PET and CT images are used both for diagnosing and staging disease and for evaluating response to therapy. We report the first performance measurements from the scanner and present some illustrative clinical studies acquired in cancer patients. **Conclusion:** A combined PET and CT scanner is a practical and effective approach to acquiring co-registered anatomical and functional images in a single scanning session.

**Key Words:** oncology; PET; CT; dual modality; image fusion

**J Nucl Med 2000; 41:1369–1379**

**T**he role of PET imaging in clinical oncology and patient care is increasing. Clinical decisions based on PET studies are changing cancer patient management by adding unique functional information to that obtained from conventional

anatomical-based modalities, such as x-ray CT and MR. Malignant cells have increased facilitated glucose transport and upregulation of hexokinase activity, and hence tumors can be identified by regions of increased glucose utilization (1). The PET tracer FDG, a glucose analog, is used to image glucose metabolism in patients. Focal areas of abnormally increased FDG uptake are considered suspicious for malignant disease, particularly as metabolic changes often precede the morphological changes associated with disease (2). Disease management will depend on the tumor type, the extent and aggressiveness of the lesion, and on local and distant metastases identified at the time of presentation. Therefore, whole-body FDG PET scanning, which can be used to diagnose and stage primary malignancy and to localize disseminated, metastatic disease in almost any region of the body, is becoming a standard procedure for imaging cancer (3).

One area in which FDG PET can play a significant role is in establishing response to treatment (1). Current procedures to monitor therapy use mainly anatomical imaging modalities, such as CT, even though metabolic changes in tumors may occur earlier than, or even instead of, anatomical size changes. A significant metabolic change can be established by comparing uptake values from pre- and posttreatment scans, although such comparisons can only be made accurately on attenuation-corrected, quantitative PET images. Attenuation correction for whole-body scanning has generally been problematic because of the increase in image noise from the transmission scan and the increase in total scan duration (emission plus transmission), which may be difficult for certain patients to tolerate for up to 1 h at a time. Therefore, many clinical readings are still performed on images uncorrected for attenuation.

A difficulty for the interpretation of FDG PET scans, particularly in the abdomen, is the absence of identifiable anatomical structures. The low contrast and low resolution anatomy visualized in the PET scan is insufficient for precise anatomical localization of foci of abnormal uptake. However, localization of increased FDG uptake to a specific organ or structure can be important when decisions affecting the diagnosis, staging, and treatment of the patient are to be made. The significance of additional anatomical information

Received Jul. 7, 1999; revision accepted Sep. 21, 1999.

For correspondence or reprints contact: David W. Townsend, PhD, PET Facility, Department of Radiology, University of Pittsburgh, 200 Lothrop St., Pittsburgh, PA 15213.

from CT has been recognized in oncology (4), but computer algorithms to co-register functional and anatomical images, although successful for relatively fixed organs such as the brain (5), are less satisfactory for internal abdominal organs that can move independently between scans. In such situations, no linear transformation exists to align the 2 sets of images. Nevertheless, attempts have been made to co-register independently acquired PET and CT images in the thorax and abdomen (6,7), and some success has been achieved by using reference markers and by operator intervention to guide the alignment (8). However, a definitive solution to this problem is to acquire both functional (PET) and anatomical (CT) images sequentially with a single scanner, without removing the patient from the bed.

This article describes the design and performance of a novel combined PET/CT scanner. Precisely co-registered anatomical and functional images can be acquired in a single scanning session, offering the potential for increased diagnostic accuracy. Patient positioning, attenuation correction, and scatter correction are based on the CT transmission images. The CT scan can be acquired postinjection without contamination from the injected activity, thus improving patient comfort and throughput. The combined PET/CT scanner has recently been installed in a hospital environment and is undergoing clinical evaluation. Three patient studies are presented to illustrate the scanner performance for applications in clinical oncology.

## MATERIALS AND METHODS

### Design Concept

The PET/CT scanner is based on the combination of a spiral CT scanner, a Somatom AR.SP (Siemens, Iselin, NJ), with the PET components from a rotating partial-ring tomograph, an ECAT ART scanner (Siemens). Both the PET and CT components are mounted on the same assembly, with the PET components on the reverse side of the rotating support of the CT scanner, as shown schematically in Figure 1A. The entire assembly is housed inside a single gantry, with the centers of the 2 tomographs offset axially by 60 cm. The bed is installed at the front of the combined gantry and is used for both the PET and CT imaging. Bed travel allows dual-modality PET and CT images to be acquired for an axial extent of 100 cm,

sufficient to cover the range from chin to lower thigh in most patients.

The CT is a third generation helical scanner, a Somatom AR.SP (Fig. 1B). Compared with single-slice CT, helical CT acquires multiple axial slices by a continuous motion of the patient bed. This results in shorter scan times and lower overall dose to the patient. Some relevant design parameters of the Somatom AR.SP are summarized in Table 1. The scanner has a metal ring M-CT 141

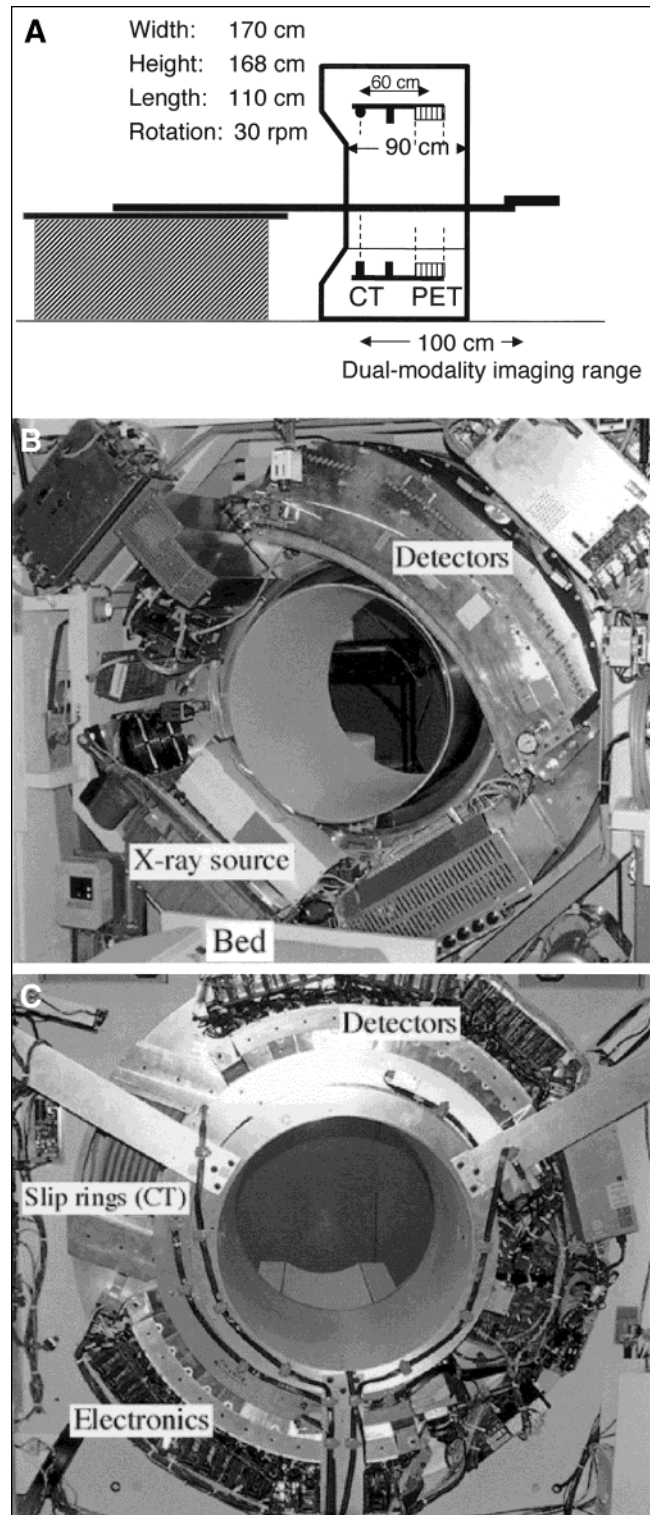


**FIGURE 1.** (A) Schematic of design concept of combined PET/CT scanner. PET components are mounted on aluminum disk attached to back of rotating CT scanner assembly. Centers of fields-of-view of PET and CT (vertical lines) are 60 cm apart. Combined PET/CT gantry is 110 cm deep, 170 cm high, and 168 cm wide. PET and CT data can be acquired over 100 cm axial range of patient. (B) Front view of Somatom AR.SP CT scanner (and front of combined PET/CT scanner) showing x-ray tube housing and x-ray detector assembly. Part of patient bed pallet also is seen. Note that space between x-ray tube and x-ray detectors is insufficient to accommodate 2 opposing ECAT ART detector arrays. (C) View from rear of PET/CT gantry showing PET detector arrays and electronics; ART detector electronics were rotated sideways 90° to fit within CT gantry dimensions. Mechanical slip rings of CT also are labeled. Other modifications are described in text.

**TABLE 1**  
Design Characteristics of the Somatom AR.SP  
(CT) Components

Component	Characteristics
Tube voltage	110, 130 kV <sub>p</sub>
Tube current	63, 83, 105 mA
Scan time per slice	1.3, 1.9 s
Slice thickness	1, 2, 3, 5, 10 mm
Gantry aperture	600 mm
Focus to isocenter	890 mm
Fan beam opening	52.2°
Transaxial field of view	450 mm

tube that produces x-ray spectra of 110 kV<sub>p</sub> or 130 kV<sub>p</sub> with a 6.5 mm Al-equivalent filter. The tube is operated with a flying spot, and, thus, 1024 detectors can be read from 512 xenon gas-filled Quantilarc chambers. The x-ray tube, cooling system, detectors, and readout electronics are all mounted on the rotating support of the CT scanner. The packing density of these components precludes the possibility to mount the PET detectors on the same side of the rotating support as the CT. Instead, the PET components are mounted to the rear of the CT support ring, on a separate aluminum annulus attached to the CT support. The PET components include the detectors and electronics, coincidence processor and the optically coupled data transmitters. An asynchronous motor rotates the entire assembly of PET and CT components at 30 rpm.

The PET detectors are standard ECAT ART components. The ECAT ART is a partial-ring, rotating tomograph comprising dual arrays of BGO block detectors. Each array consists of 11 blocks (transaxially) by 3 blocks (axially), covering an arc of 83°. The detector arrays are not symmetrically opposed (Fig. 1C) but are offset by 15° to increase the effective diameter of the transaxial field of view to 60 cm without requiring additional detector blocks. The detector blocks are 54 mm × 54 mm × 20 mm in size, cut into 8 × 8 crystals each of dimension 6.75 mm × 6.75 mm × 20 mm. Thus, the axial field of view is 16.2 cm (24 partial rings of 6.75 mm). Additional shielding of the PET components from out-of-field activity is provided by arcs of lead, 2.5 cm thick, mounted on both sides of the detector assembly and projecting 8.5 cm into the field of view beyond the front face of the detectors. Some basic design parameters of the ECAT ART components in the combined PET/CT tomograph are summarized in Table 2.

The entire rotating assembly is housed within a single gantry 170 cm wide and 168 cm high. As shown in Figure 1A, the overall tunnel length is 110 cm, with a 60 cm axial displacement between the centers of the CT and PET imaging fields of view. As a consequence of the extended length of the gantry, the tilt capability

**TABLE 2**  
Design Characteristics of the ECAT ART (PET) Components

Component	Characteristics
BGO block size	54 × 54 × 20 mm
Detector dimensions	6.75 × 6.75 × 20.0 mm
Crystal rings	24 axial
Axial field of view	162 mm
Detector ring diameter	824 mm
Image plane spacing	3.375 mm
Transaxial field of view	600 mm

of the CT was disabled. A new, strengthened tunnel cover extending from the CT field of view to the rear gantry support was installed. The lasers for the PET imaging volume and the CT encoder are mounted on the outer surface of the cylindrical tunnel. The encoder operates optically, with a copper ring containing 2048 slots passing through the encoder slit. The position information of the x-ray tube is obtained from the number of angular pulses generated by the slotted ring running through the optical encoder light switch as the assembly rotates. The zero position of the x-ray tube is determined from an index slot on the encoder ring. The CT frequency controller was adjusted to take into account the slower acceleration of the gantry that was due to the additional load of the PET components. The positional information from the CT encoder is shared with the ART communication controller so that the lines of response (LORs) from the PET acquisition are correctly assigned in the sinogram.

Power supply and data transfer to and from the PET and CT components follow separate paths. The input voltage for the x-ray tube is transformed from 110 V to 500 V outside the gantry and transmitted over mechanical slip rings. Power and serial communications to the ART components are transmitted over a different set of mechanical slip rings mounted with the ART detector arrays. High-speed digital data transfer from the ART is by optical transmission.

As with the standard ART scanner, the combined PET/CT scanner rotates continuously, eliminating the need for additional gantry cooling for the PET components. Fans start automatically if, for any reason, gantry rotation is halted. The CT scanner is cooled by 2 fans in the upper corners of the gantry that operate at all times. The x-ray tube is oil cooled.

### Bed Support

The Siemens CT bed and pallet, mounted to the front of the scanner as shown schematically in Figure 1A, is used to support the patient. Subjects up to 200 kg can be supported and positioned in the gantry to an accuracy of ±0.5 mm. To position the patient in both the CT and PET imaging fields, extended bed travel is required in addition to a support mechanism to prevent vertical deflection of the bed. The extended bed travel is required because of the 60 cm axial displacement between the CT and PET imaging fields of view. The use of an extended pallet allows an axial range of 100 cm (Fig. 1A) to be scanned by both CT and PET, sufficient to cover most patients from chin to upper thigh. To ensure accurate alignment between the 2 imaging modalities, the patient bed should be supported throughout the length of the tunnel.

### Singles Transmission Sources

To allow the combined scanner to be operated as a PET scanner only, additional transmission sources were incorporated into this prototype design. Dual, 550 MBq <sup>137</sup>Cs sources are mounted at opposite ends of the 2 PET detector arrays and transmission data are acquired in singles mode (9–11). The availability of singles transmission sources also enables a comparison to be made between CT-based attenuation correction factors and standard PET attenuation correction factors.

### PET/CT Image Processing

The CT and PET components of the combined scanner are operated independently from separate consoles. The Somatom CT console, a SUN workstation, is used for CT image acquisition and reconstruction, and it also can be used for image display and evaluation, such as measurements of tumor size.

The  $512 \times 512$  CT images are transferred over an Ethernet connection to the PET console, where combined PET/CT image processing is performed. The PET console comprises a 300-MHz UltraSparc processor with 1 Gbyte RAM, a 2 Gbyte local disk, and a 9 Gbyte external disk. Before PET image reconstruction, the emission sinogram data are corrected for scatter and attenuation. Attenuation correction is based on a rescaling of the CT image (12) and scatter correction on a single scatter model (13). PET image reconstruction of the corrected 3-dimensional sinogram data is based on the Fourier rebinning algorithm FORE (14) followed by 2-dimensional iterative reconstruction using the ordered-subset EM approach (OSEM) (15). The specific implementation of the FORE + OSEM reconstruction procedure has been described elsewhere (16).

The reconstructed PET and CT images are viewed in the pixel resolution ( $512 \times 512$ ) of the CT image on the PET console. A tool has been developed to display transverse, coronal, and sagittal sections of the PET and CT image volumes, either adjacently with linked cross-hairs or in fused mode with the PET images superimposed on the CT images. For fused image display, an interlaced pixel approach (17) is used with CT images in grayscale and the PET images superimposed in color (hot metal). The display scale of each image in both separate and fused mode can be adjusted independently. Zooming and region-of-interest capabilities are also provided.

### Operating Characteristics

The performance of BGO-based PET detectors is affected by temperature fluctuations within the scanner environment (18). Temperature fluctuations inside the combined PET/CT gantry caused by heat dissipation from the operation of the x-ray tube could be significantly greater than normal variations within the controlled gantry environment of current PET scanners. To investigate such effects, remote temperature sensors were placed at 4 locations within the combined gantry, 2 in opposite corners on the CT side and 2 in opposite corners on the PET side. Measurements were made of internal gantry temperature changes as a function of the operation of the CT scanner. Temperature readings were taken for all 4 sensors every 30 min for a period of 6 d. The PET and CT detector assembly was rotated each day for 12 h. For the first 4 d, there was no operation of the x-ray source to determine the temperature stability of the gantry during rotation of the detectors. On day 4, a sequence of CT scans of a uniform cylinder was performed delivering about 4000 mAs in total. On day 5, an extended series of both single and spiral CT scans was performed delivering a total of about 10,000 mAs.

Measurements of radiation dose delivered to the patient during a spiral CT scan were made using an MDH 9015 electrometer with a 10 cm pencil ionization chamber. Cylindrical phantoms of 15 cm and 30 cm diameter acrylic were used to simulate head (and extremities) and whole body. The multiple scan average dose (MSAD) at a depth of 1 cm was measured for typical CT scan parameters. Isodose curves for exposure levels around the tomograph were also obtained using an acrylic body phantom. To comply with radiation safety regulations and minimize exposure to personnel, the scanner room was modified to incorporate a lead glass window and lead shielding on the walls and access door.

### Performance Measurements

The performance characteristics of the PET and CT components combined were anticipated to be the same as the performances of

the ECAT ART and Somatom AR.SP, respectively. A summary of the performance of the ECAT ART based on the standard NEMA protocol (19) can be found elsewhere (20,21). To verify that the ART components in the combined scanner have equivalent performance to a commercial ECAT ART, spatial resolution, energy resolution, scatter fraction, and counting rate performance were measured according to the NEMA standards.

The performance of the CT components was evaluated according to standard procedures for clinical CT scanners. These procedures include determining the attenuation values for air and water, and measurements of image pixel noise and spatial resolution. The attenuation value of water was measured using the test protocol of the Somatom AR.SP. A 20 cm diameter, water-filled cylinder was placed in the center of the field of view and images were acquired at 110 kV<sub>p</sub> and 130 kV<sub>p</sub>. The mean pixel value and standard deviation were calculated for a circular region of interest covering 80% of the area of the water phantom. A similar measurement was performed with no phantom in the field of view to determine the attenuation value for air. The values for water and air are defined to be 0 HU (Hounsfield units) and -1000 HU, respectively, and should be independent of the x-ray tube voltage.

The water phantom then was repositioned in the center of the field of view and images again were acquired at 110 kV<sub>p</sub> and 130 kV<sub>p</sub>. Mean CT numbers were determined for five 4 cm diameter, circular regions of interest, positioned with 1 central region of interest and 4 others equally spaced peripherally. The absolute value of the difference between the average CT numbers of the central test area and the CT numbers of the 4 peripherally-placed regions of interest is then the homogeneity at 110 kV<sub>p</sub> and 130 kV<sub>p</sub>. The spatial resolution is determined by scanning a phantom comprising an air-filled cylinder with a thin metal wire along its major axis, positioned parallel to the main scanner axis. CT resolution is expressed in line pairs per cm.

For clinical, attenuation-corrected, whole-body imaging with FDG, it is important to acquire the transmission data postinjection to avoid having the patient occupying the scanner for the full 60 min uptake period required for FDG. To verify that the CT images are unaffected by the presence of positron-emitting activity in the patient, spiral CT images were acquired for two 20 cm diameter resin-filled cylinders, one containing no radioactivity and a second cylinder containing 130 MBq <sup>68</sup>Ge/<sup>68</sup>Ga. The CT scans were acquired on the PET/CT scanner with a tube voltage of 130 kV<sub>p</sub>, 160 mAs and with a slice width of 10 mm. Contiguous CT images were reconstructed, and 18 cm diameter regions of interest were centered over the cylinder in each slice. The region-of-interest mean and standard deviation for the cylinders with and without activity were compared to determine any effects that might be due to the activity in the cylinder and that would suggest emission contamination of the CT scan.

In a second study, three 5 cm diameter cylindrical inserts containing air and spongiosa and cortical bone-equivalent plastic were positioned in a 20 cm diameter, water-filled cylinder. Spiral CT images of the phantom were acquired in the Somatom AR.SP, without activity (preinjection) and with an activity concentration of 3.7 kBq/mL (postinjection) in the main compartment of the cylinder. The CT was acquired at 130 kV<sub>p</sub>, 200 mAs, and with a 3 mm slice width and a pitch of 1.6. Contiguous CT images were reconstructed and circular, and 2.5 cm diameter regions of interest were placed over the inserts and the water cylinder. As for the previous study, the region-of-interest mean and SD were compared for each insert pre- and postinjection.

## Acquisition Protocols for Clinical Imaging

For clinical imaging, a typical PET/CT acquisition protocol begins with a 260 MBq injection of FDG and a 60 min uptake period. The patient is positioned in the scanner with the first transaxial section to be imaged aligned with the field of view of the CT. An initial scout scan (topogram) is performed to determine the axial range of the spiral scan. The maximum axial extent of a single spiral scan depends on the defined slice width and pitch. The total axial length to be scanned is subdivided into contiguous, 15 cm long segments. The spiral scan of each segment typically takes about 40 s, and x-ray tube cooling sometimes may be required between segments. Patients are asked to hold their breath during the CT scan. For patients who cannot hold their breath for 40 s, either shorter axial spirals are selected or the patients are instructed to breathe shallowly. The total time for the complete CT scan is 5–10 min. Once the spiral scans covering the full axial length are completed, the patient bed is moved to the start position of the multibed PET acquisition, and the PET scan is initiated. An emission scan time of 6–10 min per bed position is selected depending on the number of bed positions, resulting in a total PET scan duration of 45–60 min. Typically, an axial overlap of 4 cm is used between contiguous bed positions.

## RESULTS

### Operating Characteristics

The results of the temperature measurements are summarized in Figure 2. Measurements were made over a period of 6 d. The graph in Figure 2 shows that the temperature

readings in the upper and lower parts of the PET scanner remained essentially constant during the first 96 h of the measurement period. Mean temperatures in the upper and lower parts were  $26.8^{\circ}\text{C} \pm 0.9^{\circ}\text{C}$  and  $27.1^{\circ}\text{C} \pm 1.0^{\circ}\text{C}$ , respectively. The measurements on the CT side of the scanner showed a slow steady decrease of about  $1^{\circ}\text{C}$  over the same period; mean temperatures in the upper and lower parts were  $24.2^{\circ}\text{C} \pm 0.9^{\circ}\text{C}$  and  $25.3^{\circ}\text{C} \pm 1.0^{\circ}\text{C}$ , respectively. During the first 96 h, temperature changes were due only to changes in ambient temperature and to changes related to the rotation of the gantry that occurred for 12 h each day. At the end of both day 4 (96 h) and day 5 (122 h), the average temperature on the CT side increased to  $26.0^{\circ}\text{C} \pm 0.8^{\circ}\text{C}$  and  $27.0^{\circ}\text{C} \pm 1.0^{\circ}\text{C}$  in the upper and lower corners of the gantry, with similar temperature increases on the PET side, reaching  $28.0^{\circ}\text{C} \pm 0.8^{\circ}\text{C}$  and  $28.4^{\circ}\text{C} \pm 0.8^{\circ}\text{C}$ . Thus, the temperature increase on the PET side that was due to the operation of the x-ray tube was  $\sim 1^{\circ}\text{C}$ . A gradual decrease in temperature was noted after the x-ray source was turned off.

X-ray dose measurements are summarized in Table 3. The measurements were made with an acrylic head and body phantom and represent the single organ dose at a depth of 1 cm below the skin surface. The x-ray tube was operated at scan conditions similar to those encountered in a clinical patient scan. Isodose curves are shown in Figure 3, representing constant exposure for a tube current product of 1000

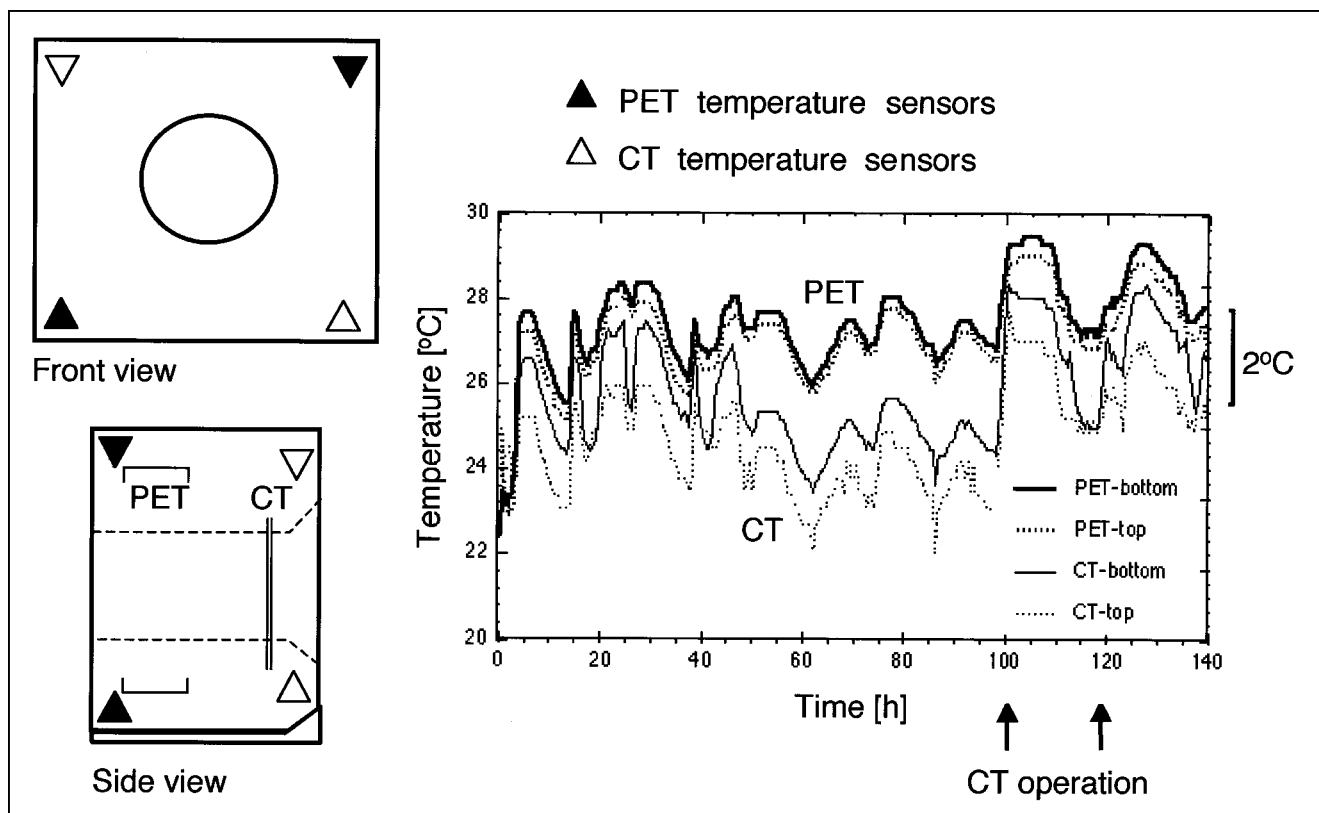


**FIGURE 2.** Gantry temperature ( $^{\circ}\text{C}$ ) measured over 6 d. Sensors were placed in top left and bottom right corners in front (CT) and rear (PET) of PET/CT gantry. Between hours 0 and 144, gantry was rotated for 12 h every day. Hours 0–95: no x-ray exposure; hour 99: x-rays on ( $\sim 4,000$  mAs); hour 120: x-rays on (10,000 mAs).

**TABLE 3**

Multiscan Average Dose (MSAD) Measured for AR.SP at 1 cm Below Skin Surface for Spiral CT Scans

Scan	Tube voltage (kVp)	Flux (mAs)	MSAD (R)
Head	130	160	4.1
Body	110	200	2.1
Body	130	200	2.9
Extremity	110	160	2.8

Slice widths for head, body, and extremity scans were 10 mm, 5 mm, and 3 mm with pitches of 1, 1.6, and 1.7, respectively.

mAs, equal to 5 scans at 100 mA with a 2 s scan time. The curves are skewed to the rear of the scanner and spread out to the front as a consequence of the asymmetric distribution of scattering media in the gantry.

**Performance Measurements**

The counting rate performance of the ECAT ART can be improved significantly by reducing the block integration time from 768 ns to 384 ns, without any observable degradation in other performance parameters, such as spatial and energy resolution (21). Therefore, the ART components of the combined scanner are operated with a block integration time of 384 ns. Standard performance measurements for the ART components in the combined scanner are summarized in Table 4. The results were comparable with those for the standard ART scanner operated with a block integration time of 384 ns (21). The corresponding standard performance parameters for the Somatom AR.SP scanner are summarized in Table 5. Again, no degradation in performance was observed compared with a standard AR.SP.

The design of the prototype with the PET and CT components mounted on opposite sides of the aluminum

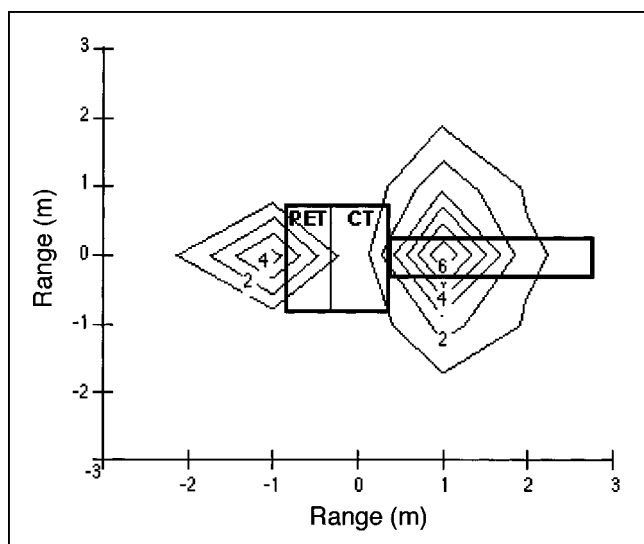


**FIGURE 3.** Isodose curves in mR for 1,000 mAs scan measured in vicinity of PET/CT scanner.

**TABLE 4**

Performance of Scanner PET Components

Component	Performance
Transaxial spatial resolution	
at $r = 0$ cm	$6.2 \pm 0.3$ mm
at $r = 10$ cm	$6.5 \pm 0.1$ mm
Axial spatial resolution	
at $r = 0$ cm	6.0 mm
Sensitivity	8.4 cps/Bq/mL
Scatter fraction	$0.36 \pm 0.02$
Maximum NEC	39.5 kcps (at 18 kBq/mL)

Measurements based on NEMA protocol (19) with 384 ns block integration time and 12 ns coincidence time window.

support minimizes potential interference between the 2 imaging systems. The PET detectors are never exposed directly to the x-ray flux, and the operation of the CT has no residual effect on the photomultiplier tube gains. The PET components can be operated immediately after the acquisition of the CT scan without requiring any recovery time. However, the PET and CT components cannot acquire data simultaneously because of the high flux of scattered CT photons incident on the PET detectors that result in high levels of randoms and dead time caused by pulse pile-up. In view of the short time required for the CT scan, simultaneous operation of the PET and CT scanners is not considered necessary.

**Acquisition Protocols**

The importance of postinjection transmission scanning has been stressed previously. The aim is to avoid having the patient occupy the scanner throughout the FDG uptake period, which would reduce patient throughput and increase the likelihood of patient movement between the transmission and emission scans. For the combined PET/CT scanner, postinjection transmission implies that the CT images must be unaffected by the presence of radioactivity in the patient. As described previously, 16 transverse CT sections were imaged along the axial length of a 20 cm diameter, uniform, resin-filled cylinder both without and with <sup>68</sup>Ge activity (~ 21 kBq/mL) in the cylinder. The mean CT number within a circular region of interest placed on the image of the

**TABLE 5**

Performance of CT Components

Transaxial spatial resolution	0.45 mm (at 1.9 s scan time)
CT value of air	$-1002 \pm 10$ HU
CT value of water	$-2 \pm 4$ HU
Cross-field uniformity	$<0.5$ HU (20 cm water cylinder)
Contrast scale	$(1.90 \pm 0.03) \cdot 10^{-4}$
Contrast resolution	2.5 mm/5 HU/1.9 s

Measurements based on standard service procedures for Somatom AR.SP. Siemens factory measurements of contrast scale and contrast resolution.

cylinder in each transaxial plane is plotted in Figure 4, both without and with activity in the cylinder. No contamination of the CT numbers by the additional activity in the cylinder is observed. The results of imaging the cylindrical phantom with the inserts are similar. The mean CT numbers for regions of interest placed over the inserts are summarized in Table 6. As with the previous study, the CT numbers in the 3 inserts do not change in the presence of activity in the cylinder.

### Clinical Studies

To illustrate the imaging of oncology patients on the combined PET/CT scanner, 3 representative case studies are presented. In each case, the patient was injected with 260 MBq FDG, and an uptake period of 60 min was allowed before commencing the first spiral CT scan. For the patient studies presented here, spiral CT scans were acquired at 130 kV<sub>p</sub> and 200 mAs with a slice width of 10 mm and a pitch of 1.5, unless stated otherwise. Contiguous CT images are reconstructed with a slice width of 3.4 mm corresponding to the default slice width for the PET scanner. The studies are presented in Figures 5–7. For each patient study, representative sections of the CT and PET volume images are displayed as (A) the CT image, (B) the corresponding PET image, and (C) the fused PET and CT image.

*Case 1.* This is a 78-y-old man with a history of T2, N2 squamous cell carcinoma of the right lung. A recent CT scan had demonstrated an increase in size of the right upper lobe mass, without lymphadenopathy. Metastatic work-up was negative preoperatively. The patient was referred for a PET/CT scan that was performed over the thorax. The PET scan duration was 8 min per bed position. The images for this patient are presented in Figure 5. A large isodense mass in the upper lobe of the right lung appears on the fused image as a highly metabolic rim surrounding a necrotic center.

*Case 2.* A 69-y-old man presented with a 6-w period of dysphagia and odynophagia. A barium swallow examination was abnormal. He was diagnosed with a hiatal hernia and a distal esophageal defect just superior to the hernia. An

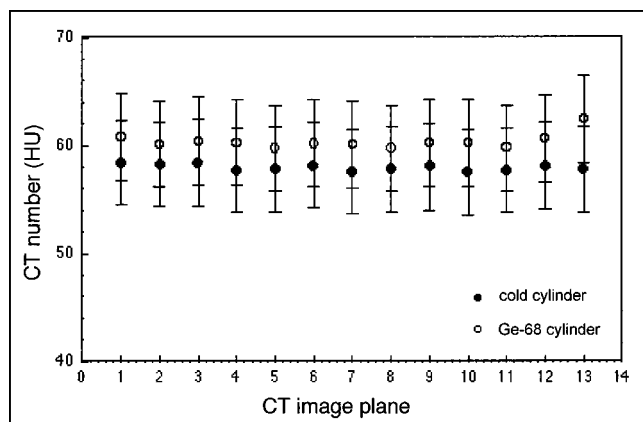


**FIGURE 4.** Mean region-of-interest values (HU) from set of transaxial CT images of cold (nonactive) and radioactive (130 MBq <sup>68</sup>Ge) resin-filled uniform cylinder.

**TABLE 6**

Attenuation Measurements Derived from CT Scans of 3 NEMA Phantom Inserts With and Without Emission Activity Contamination of 3.7 kBq/ml of <sup>18</sup>F Simulating Preinjection and Postinjection CT Scans

Insert	Preinjection	Postinjection
Air	-997.5 ± 0.8	-998.4 ± 0.8
Spongiosa	319.9 ± 0.6	319.0 ± 1.0
Cortical	1389 ± 3	1389 ± 3

Mean region-of-interest values (HU) were calculated from the central 37 transaxial image planes. Spiral CT scans were acquired at 110 kVp, 160 mAs, 3 mm slices, and a pitch of 1.6.

esophagogastroduodenoscopy showed a malignant stricture at 36–40 cm and a duodenal polyp. The pathology report identified a signet-ring shaped adenocarcinoma. The patient was referred for a PET/CT scan, which was performed over the thorax. The PET scan duration was 10 min per bed position. The PET/CT images are shown in Figure 6. The fused image (Fig. 6C) clearly shows an area of increased FDG uptake in the lymph node.

*Case 3.* A 38-y-old woman with a history of unresectable pancreatic carcinoma was diagnosed in February 1998. A laparoscopy performed after placing a stent revealed liver metastases. The patient was referred for a PET/CT scan in August 1998. A whole-body scan was performed covering the thorax and abdomen. The PET scan duration was 10 min per bed position. The PET images (Fig. 7B) showed focal uptake in the abdomen that, from the fused image (Fig. 7C), was seen to be located in the pancreas; the uptake had an SUV of 5.3. Primary pancreatic cancer was confirmed for this patient during exploratory surgery.

### DISCUSSION

The concept of dual-modality devices is not new. Lang et al. (22) developed a prototype CT/SPECT scanner using the same high-purity germanium detector array for both x-ray and single-photon imaging. More recently, Hasegawa et al. (23) developed a CT/SPECT scanner by combining a commercial gamma camera with a CT scanner, and the device has been used for a small number of clinical studies. Interest in MR as the anatomical imaging modality led to the design of the first combined PET/MR scanner (24). Because of the significant difficulties of working within a high magnetic field, restricted volume environment, this approach has been limited to a single ring of PET detectors with an aperture suitable only for small animal imaging. Finally, a combined PET/SPECT detector is under development at CTI PET Systems (Knoxville, TN) based on a hybrid crystal comprising 2 scintillators, 1 for SPECT and 1 for PET. For SPECT imaging, conventional sodium iodide is used, whereas the recently discovered scintillator lutetium oxyorthosilicate (LSO) (25) is used for detecting 511 keV photons.

The development of a combined PET and CT scanner is

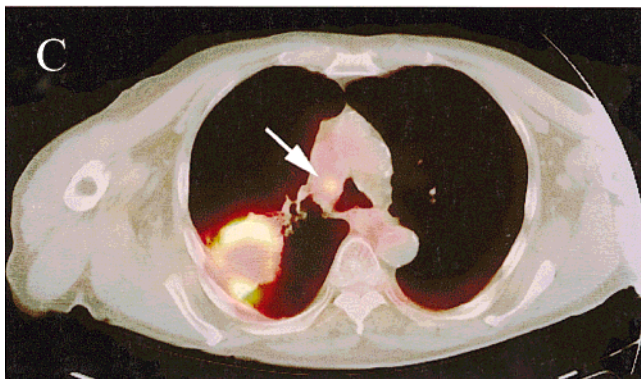
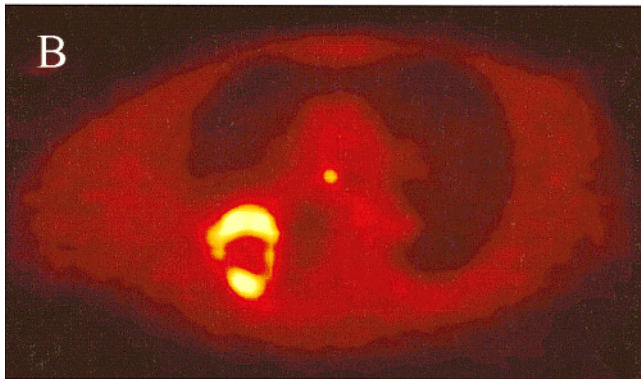


**FIGURE 5.** A 78-y-old man with squamous cell carcinoma of the lung. (A) Large isodense mass seen on CT appears on (B) PET scan as a hypermetabolic rim of increased FDG uptake, with necrotic center. (C) Fused image shows good alignment of 2 modalities. Lymph node in mediastinum (arrow) also demonstrated increased FDG uptake.

targeted primarily at oncology studies in the thorax and abdomen, although it also shows promise in cases of head and neck cancer. Whole-body oncology scans are performed to stage primary disease, evaluate nodal involvement, and identify metastatic spread to other organs. The lack of anatomical information in FDG PET scans frequently complicates interpretation, and considerable difficulty is encountered in accurately assigning functional abnormalities to specific anatomical structures. The potential for more tumor-specific tracers may eliminate even the low-resolution anatomical details discernible in FDG scans.

CT scans provide high-resolution, anatomical images that, in principle, can be aligned with the corresponding PET

scan. Mathematical registration algorithms that are generally successful for the brain encounter more difficulty, however, in the rest of the body because of the movement of internal organs, differences in the profiles of the beds, and the lack of anatomical detail on either the PET emission or transmission scans. The use of external or internal reference markers does not resolve alignment problems resulting from variability in stomach and bowel contents and other uncontrolled internal physiological changes. The combined PET/CT scanner addresses these issues by acquiring both anatomical and functional images in the same scanner, sequentially and closely spaced in time, and without moving the patient between the 2 scans.

One aspect of this design, as shown in Figure 1A, is that the centers of the CT and PET fields of view are separated axially by 60 cm and the overall tunnel length is 110 cm. However, horizontal movement of a well-supported patient bed ensures a common scanning range of 100 cm without vertical deflection between the PET and CT images. No problems of claustrophobia or refusal to be scanned have been encountered among the 110 oncology patients scanned

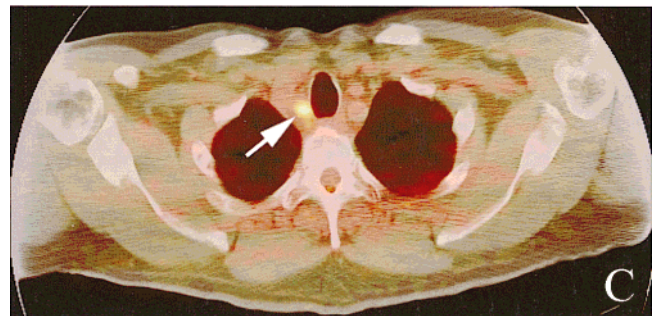
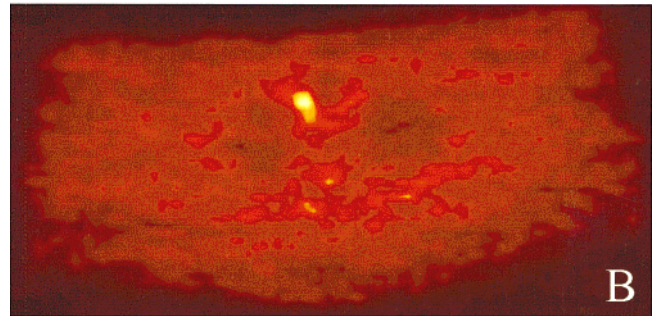
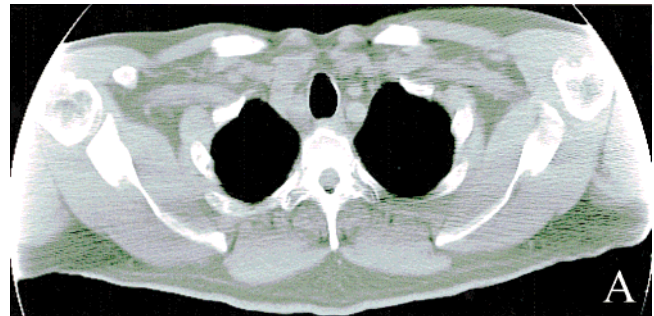


**FIGURE 6.** A 69-y-old man with diagnosed primary esophageal adenocarcinoma. (A) CT image. (B) PET image shows abnormal FDG uptake in the thorax. (C) Fused PET/CT image localizes uptake to specific lymph node (arrow).

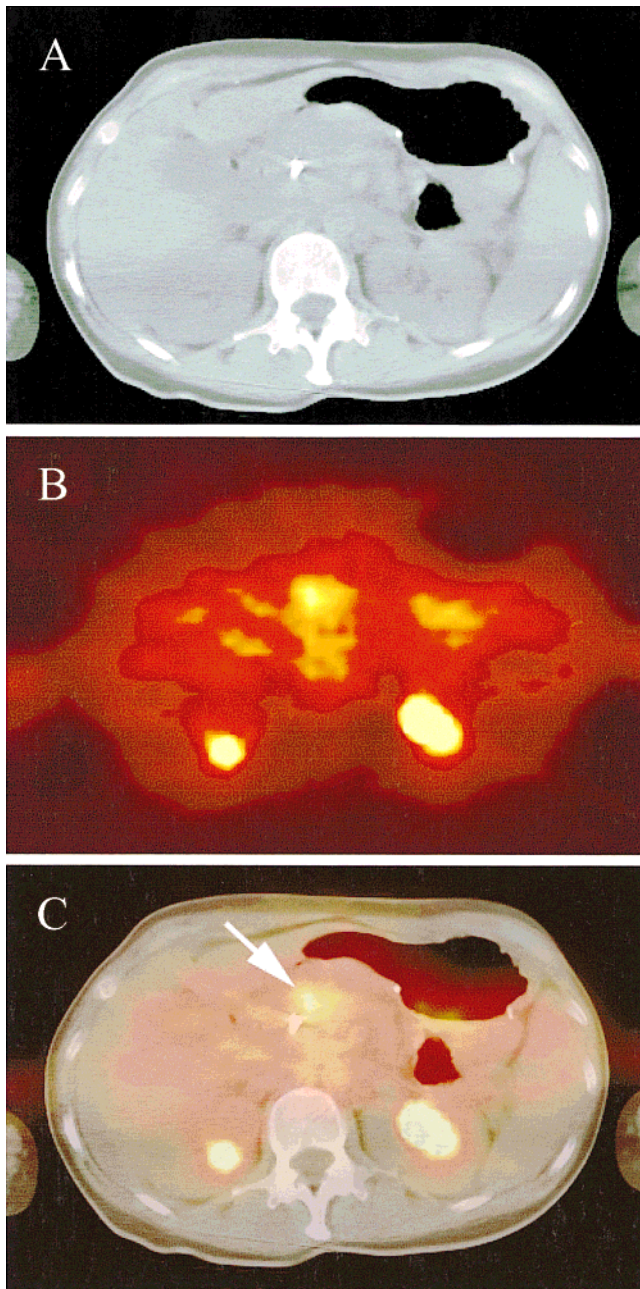


**FIGURE 7.** A 38-year-old woman with history of unresectable pancreatic cancer. Laparotomy revealed presence of liver metastases. (A) CT image. (B) Difficulty of accurately localizing FDG uptake can be seen from PET image. (C) Fused image enabled uptake to be localized to pancreas and not to transverse colon as had originally been thought.

to date. The 60 cm axial separation is actually beneficial in minimizing potential interference between the PET and CT components, such as gantry temperature changes, as shown in Figure 2 and Tables 4 and 5. The PET and CT components, therefore, perform identically to the separate commercial systems—the ECAT ART and the Somatom AR.SP. In a more integrated design where PET and CT components are mounted interleaved on the same side of the rotating

support, however, issues of interference may be more significant and will have to be re-evaluated.

For patient studies, the CT scan is acquired postinjection, immediately before the PET emission scan. The level of activity in the patient has no effect on the CT images (Fig. 4), and therefore no correction for contamination of the transmission data is required. Since the CT scan requires only about 6%–8% of the time for the PET emission scan, there is little to be gained by attempting to acquire the PET and CT scans simultaneously, particularly in view of possible artifacts in the PET data caused by CT photon pulse pile-up. Instead, a spiral CT is performed first with a continuous movement of the patient bed through the CT field of view (26). Once the spiral CT scan has been completed over the required axial range, the bed is moved into position within the PET field of view, and a PET acquisition for typically 10 min per bed position is commenced over the same axial range as the CT.

All PET images are corrected for attenuation using the CT-based correction algorithm (12). This algorithm is dependent on the choice of mean energy for the polychromatic (40 to 130 keV) CT x-ray beam. Generally, a mean energy of 70 keV is used in deriving the appropriate scaling factors. Under standard operating conditions, the photon flux from a CT scanner is a factor of at least  $10^4$  greater than that from conventional PET transmission sources. Thus, although the CT-based factors require scaling to 511 keV, compared with the standard PET transmission measurements with either rotating rod sources or point sources, the CT-based factors are essentially noiseless, even for obese, strongly attenuating patients.

The high-quality CT images also can be used to provide detailed anatomical information to the model-based scatter correction algorithm (13). In addition, the use of anatomical images as prior information to guide the PET reconstruction has been explored, and some results of this work using data from the combined PET/CT scanner have been presented by Comtat et al. (27).

Several difficulties arise from the use of the CT images for attenuation and scatter correction. One obvious difficulty is that the spiral CT scan is acquired under breath-hold conditions, whereas the PET scan is acquired continuously over a 5 to 10 min period per bed position. The expansion of the chest during the CT scan may lead to misalignment of the PET and CT images in the thorax, resulting in incorrect PET attenuation correction factors, particularly for the anterior wall. One solution is to allow the patient to breathe during multiple rotations of the CT scan, although this may reduce the quality of the CT scan and introduce motion artifacts. For the PET attenuation correction factors, the high spatial resolution of the standard CT scan is not required, and hence some nonuniform blurring of the CT scan can be applied to provide a better match between the PET and CT images. Acquiring the CT scan with the patient in a state of expiration may be a third solution in the case of a cooperative patient.

Misalignment caused by respiration and cardiac motion is

somewhat less of a problem in the abdomen. In this region of the body, combined anatomical and functional imaging is a powerful approach because of the intrinsic difficulty of interpreting PET images alone, as shown by the patient study in Figure 7. Abdominal imaging of patients with arms in the field of view often produces noticeable truncation and beam-hardening effects, particularly in obese subjects. The truncation is due to the acquisition of the CT scan with the arms of the patient in the field of view. The transaxial field of view of the CT scanner is 45 cm, and CT scans of the abdominal or thoracic region generally are acquired with the arms up. This is standard procedure with the short CT imaging times, but the 40–50 min acquisition time for PET essentially precludes imaging with the arms up except for very cooperative patients. PET imaging with the arms down requires the full, 60 cm diameter transaxial field of view of the PET scanner. Therefore, the CT scan must be corrected for the truncated projections to avoid artifacts in the CT image and biases in the CT-based attenuation correction factors. These artifacts, and the effects of beam-hardening and intravenous or oral contrast on the CT-based attenuation correction algorithm, will be addressed in a separate publication.

The effectiveness of combined PET and CT imaging is illustrated by the selected clinical cases shown in Figures 5–7. The hypermetabolic rim surrounding the large lung tumor shown in Figure 5 appears on CT as an isodense mass. Accurate co-registration was achieved in this study despite respiratory motion, and the fused functional and anatomical images potentially provide important information to guide a biopsy of the lung mass to active regions of the tumor. In the case of esophageal cancer, the PET image in Figure 6 alone shows evidence for abnormal uptake of FDG that is difficult to localize to a particular lymph node. The fused image permits precise localization to a specific node that could result in a less invasive and more efficient surgical procedure. Figure 7 illustrates the importance of combined PET and CT imaging of the abdomen. The case is that of a woman with a surgically established primary pancreatic cancer. Using CT-based attenuation correction, the focal uptake in the head of the pancreas corresponded to an SUV of 5.3. The PET images alone of this region of the body are particularly difficult to interpret owing both to the absence of anatomical landmarks (other than kidneys) and the presence of nonspecific FDG uptake in stomach, bowel, and colon. These 2 examples illustrate the utility of fused PET/CT images for accurate interpretation of FDG uptake in the thorax and abdomen, and especially where caution should be exercised when associating abnormal FDG accumulation to a malignant process.

A thorough review of the clinical cases performed on the PET/CT scanner and, in particular, an evaluation of the added value of the fused image have been published elsewhere (28).

The results from the prototype PET/CT scanner described here demonstrate the feasibility of acquiring co-registered

PET and CT images in a patient during a single scanning session. The routine availability of both functional and anatomical images from a single scan offers significant advantages over acquiring the 2 modalities separately, particularly for oncology applications in the abdomen.

## CONCLUSION

A prototype-combined PET/CT scanner was designed and built and is undergoing clinical evaluation. The scanner performs spiral whole-body CT scans and quantitative whole-body PET scans over a common axial range of 100 cm using low-noise, CT-based attenuation correction. The scans are acquired sequentially after a 60 min FDG uptake period. More than 110 patients, covering a wide range of different human cancers, have been scanned as of May 2000. The clinical results suggest an important role for combined PET and CT scanning in oncology. The acquisition of both functional and anatomical images, accurately aligned, in a single scanning session is convenient for the patient, simplifying the logistics and patient transfer. The combined PET/CT approach offers extensive possibilities for improving the diagnosis and staging of tumors, identification and localization of disseminated disease, improving radiotherapy treatment planning, and monitoring the effects of chemotherapy and radiation therapy.

## ACKNOWLEDGMENTS

The authors thank Werner Ertel and Frank Schimmel from Siemens Erlangen (Germany) for their help and advice during the design period of the PET/CT. The authors are grateful to Marsha Dachille, James Ruszkiewicz, and Donna Milko from the PET Facility, University of Pittsburgh Medical Center, for their assistance during the installation and operation of the scanner; and Carolyn C. Meltzer, MD for her assistance in reading the scans. Doug Adams, Ken Baker, Thomas Bruckbauer, John Israel, Matthias Schmand, Keith Vaigneur, and Charles Watson are thanked for their extensive contributions during the design and construction phase of the combined scanner at CTI PET Systems. The authors gratefully acknowledge the contribution of Hugo Embert, a student from the Ecole Supérieure de Chimie Physique Electronique de Lyon, to the development of the fusion image tool. This work was supported by National Cancer Institute grants CA 65856 and CA74135. David W. Townsend is a consultant for CTI PET Systems, which manufactures the ECAT ART scanner. Tony Brun, Raymond Roddy, and John Young are employees of CTI Inc. Ronald Nutt is senior vice president and director of technology for CTI PET Systems. Larry Byars owns and directs Byars Consulting of Oak Ridge, TN.

## REFERENCES

1. Smith TAD. FDG uptake, tumour characteristics and response to therapy: a review. *Nucl Med Commun.* 1998;19:97–105.
2. Strauss LG, Conti PS. The application of PET in clinical oncology. *J Nucl Med.* 1991;32:623–648.

3. Rigo P, Paulus P, Kaschten BJ, et al. Oncological applications of positron emission tomography with fluorine-18 fluorodeoxyglucose. *Eur J Nucl Med.* 1996;23:1641–1674.
4. Eubank WB, Mankoff DA, Schmiedl UP, et al. Imaging of oncologic patients: benefit of combined CT and FDG PET in the diagnosis of malignancy. *AJR* 1998;171:1101–1110.
5. Woods RP, Cherry SR, Mazziotta JC. Rapid automated algorithm for aligning and reslicing PET images. *J Comput Assist Tomogr.* 1992;16:620–633.
6. Wahl RL, Quint LE, Cieslak RD, et al. Anatomometabolic tumor imaging: fusion of FDG PET with CT or MRI to localize foci of increased activity. *J Nucl Med.* 1993;34:1190.
7. Tai YC, Lin KP, Hoh CK, Huang H, Hoffman EJ. Utilization of 3-d elastic transformation in the registration of chest x-ray CT and whole body PET. *IEEE Trans Nucl Sci.* 1997;44:1606–1612.
8. Pietrzyk U, Herholz K, Heiss W-D. Three-dimensional alignment of functional and morphological tomograms. *J Comput Assist Tomogr.* 1990;14:51–59.
9. deKemp RA, Nahmias C. Attenuation correction in PET using single photon transmission measurement. *Med Phys.* 1994;21:771–778.
10. Watson CC, Jones WF, Brun T, Veigneur K. Design and performance of a single photon transmission measurement for the ECAT ART [CD-ROM]. *IEEE Medical Imaging Conference Record.* 1998.
11. Karp JS, Muehlelehner G, Qu H, Yan XH. Singles transmission in volume-imaging PET with a <sup>137</sup>Cs source. *Phys Med Biol.* 1995;40:929–944.
12. Kinahan PE, Townsend DW, Beyer T, Sashin D. Attenuation correction for a combined 3D PET/CT scanner. *Med Phys.* 1998;25:2046–2053.
13. Watson CC, Newport D, Casey ME. A single scatter simulation technique for scatter correction in 3D PET. In: Grangeat P, Amans J-L, eds. *Computational Imaging and Vision.* Dordrecht, The Netherlands: Kluwer Academic; 1996:255–268.
14. Defrise M, Kinahan PE, Townsend DW, et al. Exact and approximate rebinning algorithms for 3D PET data. *IEEE Trans Med Imaging.* 1997;16:145–158.
15. Hudson H, Larkin R. Accelerated image reconstruction using ordered subsets of projection data. *IEEE Trans Med Imaging.* 1994;13:601–609.
16. Kinahan PE, Michel C, Defrise M, et al. Accelerated statistical reconstruction methods for PET and coincidence-SPECT whole-body oncology imaging [Abstract]. *J Nucl Med.* 1997;38:102P.
17. Rehm K, Strother SC, Anderson JR, et al. Display of merged multimodality brain images using interleaved pixels with independent color scales. *J Nucl Med.* 1994;35:1815–1821.
18. Reist HW, Stadelmann O, Kleeb W. Study on the stability of the calibration and normalization in PET and the influence of drifts on the accuracy of quantitation. *Eur J Nucl Med.* 1989;15:732–735.
19. Karp JS, Daube-Witherspoon ME, Hoffman EJ, et al. Performance standards in positron emission tomography. *J Nucl Med.* 1991;12:2342–2350.
20. Bailey DL, Young H, Bloomfield PM, et al. ECAT ART—a continuously rotating PET camera: performance characteristics, initial clinical studies and installation considerations in a nuclear medicine department. *Eur J Nucl Med.* 1997;24:6–15.
21. Townsend DW, Beyer T, Jerin J, et al. The ECAT ART scanner for positron emission tomography: 1. Improvements in performance. *Clin Pos Imag.* 1998;2:2–15.
22. Lang TF, Hasegawa BH, Liew SC, et al. Description of a prototype emission–transmission computed tomography imaging system. *J Nucl Med.* 1992;33:1881–1887.
23. Hasegawa BH, Lang TF, Brown EL, et al. Object specific attenuation correction of SPECT with correlated dual-energy x-ray CT. *IEEE Trans Nucl Sci.* 1993; NS-40:1242–1252.
24. Shao Y, Cherry SR, Farahani K, et al. Simultaneous PET and MR imaging. *Phys Med Biol.* 1997;42:1965–1970.
25. Melcher CL, Schweitzer JS. Cerium-doped lutetium oxyorthosilicate: a fast, efficient new scintillator. *IEEE Trans Nucl Sci.* 1992;39:502–505.
26. Kalender WA, Seissler W, Klotz E, Vock P. Spiral volumetric CT with single-breath-hold technique, continuous transport, and continuous scanner rotation. *Radiology.* 1990;176:181–183.
27. Comtat C, Kinahan PE, Fessler FA, et al. Reconstruction of 3D whole-body PET data using blurred anatomical labels. *IEEE Medical Imaging Conference Record.* 1999; CD-ROM.
28. Charron M, Beyer T, Bohnen N, et al. Whole-body FDG PET and CT imaging of malignancies using a combined PET/CT scanner [Abstract]. *J Nucl Med.* 1999;40:256P.